

Spectroscopy, decay properties and Regge trajectories of the B and B_s mesons*

Virendrasinh Kher^{1,2;1)} Nayneshkumar Devlani^{1;2)} Ajay Kumar Rai^{2;3)}

¹ Applied Physics Department, Polytechnic, The M.S. University of Baroda, Vadodara 390002, Gujarat, India

² Department of Applied Physics, Sardar Vallabhbhai National Institute of Technology, Surat 395007, Gujarat, India

Abstract: A Gaussian wave function is used for detailed study of the mass spectra of the B and B_s mesons using a Cornell potential incorporated with a $\mathcal{O}(1/m)$ correction in the potential energy term and expansion of the kinetic energy term up to $\mathcal{O}(\mathbf{p}^{10})$ for relativistic correction of the Hamiltonian. The predicted excited states for the B and B_s mesons are in very good agreement with results obtained by experiment. We assign B₂(5747) and B_{s2}(5840) as the 1^3P_2 state, B₁(5721) and B_{s1}(5830) as the $1P_1$ state, B₀(5732) as the 1^3P_0 state, B_{s1}(5850) as the $1P_1'$ state and B(5970) as the 2^3S_1 state. We investigate the Regge trajectories in the (J, M^2) and (n_r, M^2) planes with their corresponding parameters. The branching ratios for leptonic and radiative-leptonic decays are estimated for the B and B_s mesons. Our results are in good agreement with experimental observations as well as outcomes of other theoretical models.

Keywords: potential model, mass spectrum, decay constant, Regge trajectories

PACS: 12.39.Jh, 12.40.Yx, 13.20.Gd **DOI:** 10.1088/1674-1137/41/9/093101

1 Introduction

The last decade has been marked by noteworthy experimental progress in understanding the spectroscopy of mesons containing heavy-light quarks. In the case of the B and B_s mesons, the ground state as well as first few orbitally excited states have been well established experimentally. Other radially and orbitally excited states, however, require further experimental investigation [1–5].

In 2013, the CDF collaboration investigated the $B^0\pi^+$ and $B^+\pi^-$ invariant mass distributions using data at $\sqrt{s} = 1.96$ TeV $p\bar{p}$ collisions corresponding to an integrated luminosity of 9.6 fb^{-1} . They found evidence for a new resonance, the B(5970). The reported mass and width of the neutral state are $5978 \pm 5 \pm 12$ MeV and $70_{-20}^{+30} \pm 30$ MeV respectively. More recently, the LHCb collaboration also studied the $B^0\pi^+$ and $B^+\pi^-$ invariant mass distribution using $\sqrt{s} = 7$ and $\sqrt{s} = 8$ TeV corresponding to an integrated luminosity of 3.0 fb^{-1} . Precise measurements were made of the mass and width of the B₁(5721) and B₂^{*}(5747), as well as observing two excited

states, B_J(5840)^{0,+} and B_J(5960)^{0,+} [6, 7].

As well as the experimental observations, the states of the B and B_s mesons have already been predicted by various theoretical models. These predictions employ various relativistic or relativized quark models, potential models, the Bethe-Salpeter equation as well as constituent quark models based on the Dirac equation [2–4, 8–13]. Experimental exploration of newly observed and unconfirmed states of the B and B_s mesons motivate us to carry out a comprehensive theoretical study.

In this article, we employ a potential model, incorporating corrections to the potential energy part besides the kinematic relativistic correction of the Hamiltonian, to understand the B and B_s mesons. Using our predicted masses for the B and B_s mesons, we plot the Regge trajectories in both the $(M^2 \rightarrow J)$ and $(M^2 \rightarrow n)$ planes (where J is the spin and n is the principal quantum number). These play a vital role in identifying any new (experimentally) excited states as well as for information about the quantum numbers of the particular state [14].

In the present work, the leptonic and radiative leptonic decay widths are estimated. The radiative leptonic

Received 17 April 2017

* A. K. Rai acknowledges the financial support extended by the Department of Science of Technology, India under SERB fast track scheme SR/FTP /PS-152/2012

1) E-mail: vkhker@gmail.com

2) E-mail: nayneshdev@gmail.com

3) E-mail: raiajayk@gmail.com



Content from this work may be used under the terms of the Creative Commons Attribution 3.0 licence. Any further distribution of this work must maintain attribution to the author(s) and the title of the work, journal citation and DOI. Article funded by SCOAP³ and published under licence by Chinese Physical Society and the Institute of High Energy Physics of the Chinese Academy of Sciences and the Institute of Modern Physics of the Chinese Academy of Sciences and IOP Publishing Ltd

decay of mesons can be equal to or larger than the pure-leptonic decay, which can allow study of the effect of the strong interaction in the decay [15].

The article is organized as follows. In Section 2.1, we present the theoretical framework for the mass spectra. Section 2.2 introduces the theoretical framework for leptonic, dileptonic and radiative leptonic decay widths. The results of mass spectra, leptonic and radiative-leptonic decays are discussed in Section 3. In Section 3.1, we investigate Regge trajectories in the (J, M^2) and (n_r, M^2) planes. Finally, we present the conclusion in Section 4.

2 Methodology

2.1 Cornell potential with $\mathcal{O}(\frac{1}{m})$ corrections

For spectroscopic study of the B and B_s mesons, we employ the Hamiltonian [16–18]

$$H = \sqrt{\mathbf{p}^2 + m_Q^2} + \sqrt{\mathbf{p}^2 + m_{\bar{q}}^2} + V(\mathbf{r}), \quad (1)$$

where \mathbf{p} stands for the relative momentum of the meson, m_Q for the mass of the heavy quark, $m_{\bar{q}}$ for the mass of the light anti-quark, and $V(\mathbf{r})$ is the meson potential, which can be written as [19],

$$V(r) = V^{(0)}(r) + \left(\frac{1}{m_Q} + \frac{1}{m_{\bar{q}}} \right) V^{(1)}(r) + \mathcal{O}\left(\frac{1}{m^2}\right). \quad (2)$$

$V^{(0)}$ is a Cornell-like potential [20],

$$V^{(0)}(r) = -\frac{\alpha_c}{r} + Ar + V_0 \quad (3)$$

$V^{(1)}(r)$ in leading order perturbation theory yields

$$V^{(1)}(r) = -C_F C_A \alpha_s^2 / 4r^2 \quad (4)$$

where $\alpha_c = (4/3)\alpha_S(M^2)$, $\alpha_S(M^2)$ is the strong running coupling constant, A is a potential parameter, V_0 is a constant, and $C_F = 4/3$ and $C_A = 3$ are the Casimir charges [19].

Here, we use the Ritz variational strategy for the study of the B and B_s mesons. In the heavy-light mesons, the confining interaction plays an important role. We employ a Gaussian wave function to predict the expectation values of the Hamiltonian [18, 21, 22]. The Gaussian wave function in position space has the form

$$R_{nl}(\mu, r) = \mu^{3/2} \left(\frac{2(n-1)!}{\Gamma(n+l+1/2)} \right)^{1/2} (\mu r)^l \times e^{-\mu^2 r^2 / 2} L_{n-1}^{l+1/2}(\mu^2 r^2) \quad (5)$$

and in momentum space has the form

$$R_{nl}(\mu, p) = \frac{(-1)^n}{\mu^{3/2}} \left(\frac{2(n-1)!}{\Gamma(n+l+1/2)} \right)^{1/2} \left(\frac{p}{\mu} \right)^l \times e^{-p^2 / 2\mu^2} L_{n-1}^{l+1/2} \left(\frac{p^2}{\mu^2} \right). \quad (6)$$

Here, L and μ represent the Laguerre polynomial and the variational parameter respectively. Using the virial theorem [17], we found the value of variational parameter μ for each state, for the chosen value of potential parameter A ,

$$\langle K.E. \rangle = \frac{1}{2} \left\langle \frac{rdV}{dr} \right\rangle. \quad (7)$$

To justify the relativistic approach for quarks within the heavy-light mesons, we expand the kinetic energy of the quarks, retaining powers up to $\mathcal{O}(\mathbf{p}^{10})$, from the Hamiltonian Eq. (1) [18]. In the virial theorem, we use a momentum space wave function to determine the expectation value of the kinetic energy part, whereas a position space Gaussian wave-function is used to determine the expectation value of the potential energy part.

Here, the center of weight mass is the expectation value of the Hamiltonian. By fixing the potential constant V_0 , α_s and A , we fitted the ground state center of the weight mass and matched it with the PDG value. The fitted potential parameters are listed in Table 1. Using the following equation, we fitted the ground state center of weight mass [23, 24]:

$$M_{SA} = M_P + \frac{3}{4}(M_V - M_P), \quad (8)$$

where M_V is a vector and M_P is a pseudoscalar meson ground state mass. Using the potential parameter listed in Table 1, we predicted the S , P , and D state wave center of weight masses of the mesons, which are tabulated in Table 3. For the nJ state comparison, we computed the center of weight mass from the respective theoretical values as [23]:

$$M_{CW,n} = \frac{\sum_J (2J+1) M_{nJ}}{\sum_J (2J+1)}, \quad (9)$$

where $M_{CW,n}$ is the center of weight mass of the n state and M_{nJ} is the meson mass in the nJ state. The hyperfine and spin-orbit shifting of the low-lying S , P and D states have been estimated by the spin-dependent part of the conventional one gluon exchange potential between the quark and anti-quark [18, 25–27]

$$V_{SD}(\mathbf{r}) = \left(\frac{\mathbf{L} \cdot \mathbf{S}_Q}{2m_Q^2} + \frac{\mathbf{L} \cdot \mathbf{S}_{\bar{q}}}{2m_{\bar{q}}^2} \right) \left(-\frac{dV^{(0)}(r)}{rdr} + \frac{8}{3} \alpha_S \frac{1}{r^3} \right) + \frac{4}{3} \alpha_S \frac{1}{m_Q m_{\bar{q}}} \frac{\mathbf{L} \cdot \mathbf{S}}{r^3} + \frac{4}{3} \alpha_S \frac{2}{3m_Q m_{\bar{q}}} \mathbf{S}_Q \cdot \mathbf{S}_{\bar{q}} 4\pi\delta(\mathbf{r}) + \frac{4}{3} \alpha_S \frac{1}{m_Q m_{\bar{q}}} \left\{ 3(\mathbf{S}_Q \cdot \mathbf{n})(\mathbf{S}_{\bar{q}} \cdot \mathbf{n}) - (\mathbf{S}_Q \cdot \mathbf{S}_{\bar{q}}) \right\} \frac{1}{r^3}, \quad \mathbf{n} = \frac{\mathbf{r}}{r}, \quad (10)$$

where $V^0(r)$ stands for the phenomenological potential. In the spin-dependent part, the first part stands for the

relativistic corrections to the potential $V^0(r)$, the second part stands for the spin-orbital interaction, the third part stands for the conventional spin-spin interaction and fourth part stands for the tensor interaction.

Table 1. Potential parameters.

meson	α_s	A/GeV^2	V_0/GeV
B	0.6675	0.118	-0.00742
B_s	0.59025	0.140	-0.0108

Mass eigenstates for heavy-light meson are constructed by jj coupling. The quantum numbers \mathbf{S}_Q and the light degrees of freedom $\mathbf{j}_{\bar{q}} = \mathbf{s}_{\bar{q}} + \mathbf{L}$ are individually conserved. Here, \mathbf{S}_Q is the heavy quark spin, $\mathbf{s}_{\bar{q}}$ is the light quark spin and \mathbf{L} is the orbital angular momentum of the light quark. The quantum numbers of the excited $L=1$ states are formed by combining \mathbf{S}_Q and $\mathbf{j}_{\bar{q}}$. For $L=1$ we have $\mathbf{j}_{\bar{q}}=1/2$ ($\mathbf{J}=0,1$) and $\mathbf{j}_{\bar{q}}=3/2$ ($\mathbf{J}=1,2$) states. These states are denoted as $^3P_0, ^1P'_1$ ($\mathbf{j}_{\bar{q}}=1/2$), 1P_1 ($\mathbf{j}_{\bar{q}}=3/2$) and 3P_2 in the case of the B and B_s meson. [18, 27]

Independently of the total spin J projection, one has

$$|^{2L+1}L_{L+1}\rangle = |J=L+1, S=1\rangle, \quad (11)$$

$$|^{2L+1}L_L\rangle = \sqrt{\frac{L}{L+1}}|J=L, S=1\rangle + \sqrt{\frac{L+1}{2L+1}}|J=L, S=0\rangle, \quad (12)$$

$$|^{2L-1}L_L\rangle = \sqrt{\frac{L+1}{2L+1}}|J=L, S=1\rangle - \sqrt{\frac{L}{2L+1}}|J=L, S=0\rangle, \quad (13)$$

where $|J, S\rangle$ are the state vectors with the given values of the total quark spin $\mathbf{S} = \mathbf{s}_{\bar{q}} + \mathbf{S}_Q$, hence the potential terms of the order of $1/m_{\bar{q}}m_Q, 1/m_Q^2$ lead to the mixing of the levels with the different $\mathbf{j}_{\bar{q}}$ values at the given J values. The tensor forces (fourth term in Equation (10)) are zero at $L=0$ or $S=0$.

The heavy-heavy flavored meson states with $J=L$ are mixtures of spin-triplet $|^3L_L\rangle$ and spin-singlet $|^1L_L\rangle$ states: $J=L=1, 2, 3, \dots$

$$|\psi_J\rangle = |^1L_L\rangle \cos\phi + |^3L_L\rangle \sin\phi, \quad (14)$$

$$|\psi'_J\rangle = -|^1L_L\rangle \sin\phi + |^3L_L\rangle \cos\phi, \quad (15)$$

where ϕ is the mixing angle and the primed state has the heavier mass. Such mixing occurs due to the nondiagonal spin-orbit and tensor terms in Eq. (10). The masses of the physical states were obtained by diagonalizing the mixing matrix obtained using Eq. (10) [27]. Charge conjugating $q\bar{q}$ into $b\bar{q}$ flips the sign of the angle and the phase convention depends on the order of coupling \mathbf{L}, \mathbf{S}_Q

and $\mathbf{s}_{\bar{q}}$. Radiative transitions are particularly sensitive to the $^3L_L - ^1L_L$ mixing angle, with predictions giving radically different results in some cases of different models [28, 29]. The values of mixing angles for the P and D states are tabulated in Table 2.

Table 2. Mixing angles θ for B and B_s mesons.

meson	$\theta_1^0 P$	$\theta_2^0 P$	$\theta_3^0 P$	$\theta_1^0 D$	$\theta_2^0 D$	$\theta_3^0 D$
B	-14.66	-15.71	-16.04	71.99	71.89	72.86
B_s	-9.97	-12.41	-13.01	72.17	72.04	71.99

In the present study, the quark masses are $m_{u/d} = 0.46$ GeV, $m_b = 4.530$ GeV and $m_s = 0.586$ GeV, to reproduce the ground state masses of the B and B_s mesons.

2.2 Leptonic, radiative leptonic and dileptonic branching fractions

To predict the leptonic branching fractions for the (1^1S_0) B mesons, we employed the formula

$$BR = \Gamma \times \tau, \quad (16)$$

where Γ (leptonic decay width) is given by [30]

$$\Gamma(B^+ \rightarrow l^+ \nu_l) = \frac{G_F^2}{8\pi} f_B^2 |V_{ub}|^2 m_l^2 \times \left(1 - \frac{m_l^2}{M_B^2}\right)^2 M_B. \quad (17)$$

For the calculation of the radiative leptonic decay $B^- \rightarrow \gamma l \bar{\nu}$ ($l=e, \mu$) width, we employ the formula [31]

$$\Gamma(B^- \rightarrow \gamma l \bar{\nu}) = \frac{\alpha G_F^2 |V_{bu}|^2}{2592\pi^2} f_{B^-}^2 m_{B^-}^3 [x_u + x_b], \quad (18)$$

where

$$x_u = \left(3 - \frac{m_{B^-}}{m_u}\right)^2, \quad (19)$$

and

$$x_b = \left(3 - 2\frac{m_{B^-}}{m_b}\right)^2 \quad (20)$$

Due to the conservation of charge, single charged lepton decays as well as decays to two muons are forbidden at the primary transition, but such types of decay occur in higher-order transitions. Due to Cabibbo-Kobayashi-Maskawa and helicity suppression, there is an expectation of very small branching fraction for the $B^0 \rightarrow \mu^+ \mu^-$ and $B_s^0 \rightarrow \mu^+ \mu^-$ compared to the dominant \bar{b} to \bar{c} transitions. Hence, one can consider dileptonic decays as rare decays. The decay width for the B_s^0 and B^0 mesons is given by [3, 32, 33]

$$\Gamma(B_q^0 \rightarrow l^+ l^-) = \frac{G_F^2}{\pi} \left(\frac{\alpha}{4\pi \sin^2 \Theta_W}\right)^2 f_{B_q}^2 m_l^2 m_{B_q} \times \sqrt{1 - 4\frac{m_l^2}{m_{B_q}^2}} |V_{tq}^* V_{tb}|^2 |C_{10}|^2 \quad (21)$$

The branching ratio for $B_q^0 \rightarrow 1^+ 1^-$ is

$$BR \rightarrow \Gamma_{(B_q^0 \rightarrow 1^+ 1^-)} \times \tau_{B_q}, \quad (22)$$

G_F is the Fermi coupling constant, f_{B_q} is the corresponding decay constant, and C_{10} is the Wilson coefficient given by [3, 34, 35].

$$C_{10} = \eta_Y \frac{x_t}{8} \left[\frac{x_t + 2}{x_t - 1} + \frac{3x_t - 6}{(x_t - 1)^2} \ln x_t \right], \quad (23)$$

where $\eta_Y (= 1.026)$ is the next-to-leading-order correction [3, 35], $\Theta_W (\approx 28^\circ)$ is the weak mixing angle (Weinberg angle) [36], and $x_t = (m_t/m_w)^2$.

The decay constants were obtained from the Van-Royen-Weisskopf formula [37]. Incorporating the first order QCD correction factor,

$$f_{P/V}^2 = \frac{12 |\psi_{P/V}(0)|^2}{M_{P/V}} \bar{C}^2(\alpha_S), \quad (24)$$

where $\bar{C}^2(\alpha_S)$ is the QCD correction factor given by [38]

$$\bar{C}^2(\alpha_S) = 1 - \frac{\alpha_S}{\pi} \left[2 - \frac{m_Q - m_{\bar{q}}}{m_Q + m_{\bar{q}}} \ln \frac{m_Q}{m_{\bar{q}}} \right]. \quad (25)$$

We calculate the leptonic branching fractions using Eq. (17), the radiative leptonic branching ratio using Eq. (18) for the B meson and the dileptonic branching ratio with corresponding decay width using Eq. (21) for the B and B_s mesons. We have taken $\tau_B = 1.638$ ps, $\tau_{B_s} = 1.510$ ps [1] and the calculated values of the pseudoscalar decay constant $f_B = 0.146(0.150)$ GeV and

$f_{B_s} = 0.187(0.203)$ GeV with(without) QCD correction using the masses obtained from Tables 4 and 5.

3 Results and discussion

The center of weight masses for the S, P and D states are estimated using Eq. (8) and Eq. (9), and the results are tabulated in Table 3. In the case of the B meson, the center of weight masses for the $1S$, $2S$, $3S$, $1P$, $2P$, $1D$ and $2D$ states are in good agreement with the outcomes of other theoretical models, whereas masses for $4S$, $5S$, $3P$ and $3D$ are somewhat overestimated. In the case of the B_s meson, the center of weight masses are in good agreement with the outcomes of other theoretical models.

The estimated mass spectra for the B and B_s mesons are tabulated in Tables 4 and 5 with the spectroscopic notation $n^{2S+1}L_J$. The mass spectra are also depicted graphically in Figs. 1 and 2. The predicted masses of the B and B_s mesons are in close agreement with experimental observations. The difference between the predicted and experimentally observed values of the mass of the B meson is 7 MeV for 1^1S_0 , 2 MeV for 1^3S_1 , 20 MeV for 1^3P_0 , 7 MeV for $1P_1$ and matches for the 1^3P_2 state. Similarly, the difference between the predicted and experimentally observed values of the mass of the B_s meson is 1 MeV for 1^1S_0 , 2 MeV for 1^3S_1 , 1 MeV for 1^3P_1 , 11 MeV for $1^3P_1'$ and matches for the 1^3P_2 state.

Table 3. S - P - D -wave center of weight masses (in GeV) of the B meson.

meson	state	μ	M_{CW}	Expt [1]	[2]	[3]	[4]	[39]	[40]	[14]	[41]
B	$1S$	0.382	5.314	5.314	5.317	5.314	5.288	5.354	5.314	5.314	5.313
	$2S$	0.279	5.942		5.932	5.819	5.903	5.926	5.942	5.902	5.842
	$3S$	0.233	6.504		6.386	6.251		6.350	6.394	6.385	6.313
	$4S$	0.206	7.036			6.647			6.778	6.785	6.347
	$5S$	0.187	7.546							7.132	
	$1P$	0.309	5.740		5.748	5.737	5.759	5.785	5.774	5.745	5.696
	$2P$	0.249	6.301		6.224	6.127	6.188	6.213	6.250	6.249	6.030
	$3P$	0.216	6.828			6.482				6.669	6.265
	$1D$	0.278	6.057		6.048	6.065	6.042	6.108	6.079	6.106	5.924
	$2D$	0.232	6.596		6.467	6.429	6.377	6.466	6.495	6.540	6.183
	$3D$	0.205	7.110			6.769					
B_s	$1S$	0.470	5.401	5.401	5.400	5.403	5.370	5.433	5.401	5.404	5.404
	$2S$	0.341	6.023		5.997	5.952	5.971	6.006	6.011	5.988	5.959
	$3S$	0.285	6.570		6.430	6.425		6.424	6.447	6.473	6.259
	$4S$	0.252	7.083			6.863			6.816	6.878	6.500
	$5S$	0.230	7.575								
	$1P$	0.376	5.835		5.827	5.838	5.838	5.858	5.851	5.844	5.805
	$2P$	0.303	6.380		6.280	6.233	6.254	6.290	6.310	6.343	6.161
	$3P$	0.264	6.889			6.603				6.768	6.413
	$1D$	0.337	6.150		6.116	6.181	6.117	6.181	6.147	6.200	6.047
	$2D$	0.283	6.668		6.513	6.626	6.450	6.539	6.546	6.635	6.323
	$3D$	0.251	7.162			6.912					

Table 4. Predicted masses (in GeV) for the B meson.

state	J^P	present work	Expt. [1]	[2]	[3]	[4]	[39]	[40]	[14]	[41]
1^1S_0	0^-	5.287	5.280 (B^0)	5.280	5.279	5.273	5.309	5.266	5.280	5.277
1^3S_1	1^-	5.323	5.325 (B^*)	5.329	5.325	5.331	5.369	5.330	5.326	5.325
2^1S_0	0^-	5.926		5.910	5.804	5.893	5.904	5.930	5.890	5.822
2^3S_1	1^-	5.947	5.961 $B(5970)$ [42]	5.939	5.824	5.932	5.934	5.946	5.906	5.848
3^1S_0	0^-	6.492		6.369	6.242		6.334	6.387	6.379	6.117
3^3S_1	1^-	6.508		6.391	6.254		6.355	6.396	6.387	6.136
4^1S_0	0^-	7.027			6.641			6.773	6.781	6.335
4^3S_1	1^-	7.039			6.649			6.779	6.786	6.351
5^1S_0	0^-	7.538								
5^3S_1	1^-	7.549								
1^3P_0	0^+	5.730	5.710 $B_0(5732)$ [43]	5.683	5.697	5.740	5.756	5.746	5.749	5.678
$1P_1$	1^+	5.733	5.726 $B_1(5721)$	5.729	5.723	5.815	5.782	5.764	5.723	5.686
$1P'_1$	1^+	5.752		5.754	5.738	5.731	5.779	5.785	5.774	5.699
1^3P_2	2^+	5.740	5.740 $B_2(5747)$	5.768	5.754	5.746	5.796	5.779	5.741	5.704
2^3P_0	0^+	6.297		6.145	6.053	6.188	6.214	6.225	6.221	6.010
$2P_1$	1^+	6.295		6.185	6.106	6.168	6.206	6.243	6.209	6.022
$2P'_1$	1^+	6.311		6.241	6.131	6.221	6.219	6.256	6.281	6.028
2^3P_2	2^+	6.299		6.253	6.153	6.179	6.213	6.255	6.260	6.040
3^3P_0	0^+	6.826			6.375				6.629	6.242
$3P_1$	1^+	6.824			6.453				6.650	6.259
$3P'_1$	1^+	6.837			6.486				6.685	6.260
3^3P_2	2^+	6.826			6.518				6.678	6.277
1^3D_1	1^-	6.016		6.095	6.104	6.135	6.110	6.114	6.119	6.005
$1D_2$	2^-	6.031		6.004	6.076	5.967	6.108	6.125	6.121	5.955
$1D'_2$	2^-	6.065		6.113	6.065	6.152	6.113	6.056	6.103	5.920
1^3D_3	3^-	6.085		6.014	6.041	5.976	6.105	6.060	6.091	5.871
2^3D_1	1^-	6.562		6.497	6.460	6.445	6.475	6.522	6.534	6.248
$2D_2$	2^-	6.575		6.435	6.440	6.323	6.464	6.532	6.554	6.207
$2D'_2$	2^-	6.602		6.513	6.429	6.456	6.472	6.476	6.528	6.179
2^3D_3	3^-	6.619		6.444	6.409	6.329	6.459	6.479	6.542	6.140
3^3D_1	1^-	7.081			6.795					
$3D_2$	2^-	7.093			6.768					
$3D'_2$	2^-	7.116			6.779					
3^3D_3	3^-	7.130			6.751					

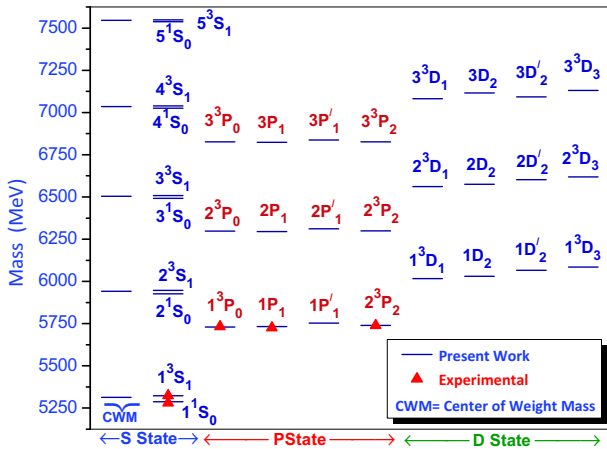


Fig. 1. (color online) Mass spectrum of the B meson.

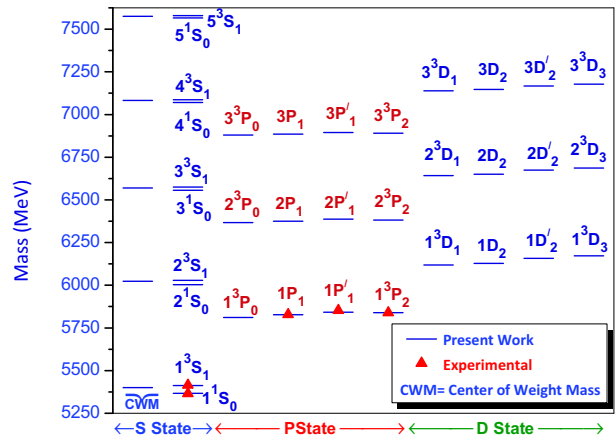


Fig. 2. (color online) Mass spectrum of the B_s meson.

The predicted leptonic branching fractions for the B meson are tabulated in Table 6. The predicted BR_μ and BR_e indicates that the predictions are in good agreement with the experimental outcomes, while BR_τ is slightly underestimated with respect to experimental observations. In the literature, various methods are used to calculate the radiative leptonic decay rate and branching ratio. In Ref. [51], the calculated branching ratio $B \rightarrow l\bar{\nu}\gamma$ is of the order of 10^{-6} in a non-relativistic quark model. In Ref. [48] with the perturbative QCD approach, it is found that the branching ratio of $B^+ \rightarrow e^+\bar{\nu}\gamma$ is of the order of 10^{-6} . In the factorization approach, it is found to be of order of 10^{-6} for the B meson [11, 49, 50, 52]. In the form factors parameterizing approach, it is found to be the order of 10^{-7} [48]. We also found a branching ratio of the order of 10^{-7} for the B meson.

Our predicted decay widths and branching ratios for

the rare leptonic decays $B_s \rightarrow l^+l^-$ and $B \rightarrow l^+l^-$, ($l = \mu, \tau, e$) are shown in Tables 7 and 8. The predicted branching ratios $B_s \rightarrow \mu^+\mu^- = 2.529 \times 10^{-9}$ and $B \rightarrow \mu^+\mu^- = 1.002 \times 10^{-10}$ are in excellent agreement with the experimental results published by CMS and LHCb [44, 46, 53]. The predicted branching ratios $B_s^0 \rightarrow e^+e^- = 5.921 \times 10^{-14}$ and $B^0 \rightarrow e^+e^- = 2.345 \times 10^{-15}$ are in good agreement with Ref. [3] (Dirac formalism), Ref. [32] (Standard Model with reduced theoretical uncertainty) and Ref. [47] (lattice results). We have also predicted the branching ratio with corresponding decay width of other rare leptonic ($l = \tau, e$) decays for the B and B_s mesons. Due to the large uncertainty in experimental observations in rare leptonic ($l = \tau, e$) decays for the B and B_s mesons, it is difficult to come to a reasonable conclusion, but our results are in relatively good agreement with the predictions by other theoretical models.

Table 5. Predicted masses (in GeV) for the B_s meson.

state	J^P	present work	Expt. [1]	[2]	[3]	[4]	[39]	[40]	[14]	[41]
1^1S_0	0^-	5.367	$5.366 B_s^0$	5.362	5.366	5.355	5.390	5.355	5.372	5.366
1^3S_1	1^-	5.413	$5.415 B_s^*$	5.413	5.415	5.416	5.447	5.417	5.414	5.417
2^1S_0	0^-	6.003		5.977	5.939	5.962	5.985	5.998	5.976	5.939
2^3S_1	1^-	6.029		6.003	5.956	5.999	6.013	6.016	5.992	5.966
3^1S_0	0^-	6.556		6.415	6.419		6.409	6.441	6.467	6.254
3^3S_1	1^-	6.575		6.435	6.427		6.429	6.449	6.475	6.274
4^1S_0	0^-	7.071			6.859			6.812	6.874	6.487
4^3S_1	1^-	7.087			6.864			6.818	6.879	6.504
5^1S_0	0^-	7.565								
5^3S_1	1^-	7.579								
1^3P_0	0^+	5.812		5.756	5.799	5.782	5.830	5.820	5.833	5.781
$1P_1$	1^+	5.828	$5.829 B_{s1}(5830)$	5.801	5.819	5.833	5.838	5.857	5.865	5.805
$1P'_1$	1^+	5.842	$5.853 B_{s1}(5850)$	5.836	5.854	5.843	5.859	5.845	5.831	5.795
1^3P_2	2^+	5.840	$5.840 B_{s2}(5840)$	5.851	5.849	5.848	5.875	5.859	5.842	5.815
2^3P_0	0^+	6.367		6.203	6.171	6.220	6.279	6.283	6.318	6.143
$2P_1$	1^+	6.375		6.241	6.197	6.250	6.284	6.306	6.345	6.153
$2P'_1$	1^+	6.387		6.297	6.278	6.256	6.291	6.312	6.321	6.160
2^3P_2	2^+	6.382		6.309	6.241	6.261	6.295	6.317	6.359	6.170
3^3P_0	0^+	6.879			6.510				6.731	6.396
$3P_1$	1^+	6.885			6.663				6.761	6.406
$3P'_1$	1^+	6.895			6.543				6.768	6.411
3^3P_2	2^+	6.890			6.622				6.780	6.421
1^3D_1	1^-	6.119		6.142	6.226	6.155	6.181	6.188	6.209	6.094
$1D_2$	2^-	6.128		6.087	6.177	6.079	6.180	6.199	6.218	6.067
$1D'_2$	2^-	6.157		6.159	6.209	6.172	6.185	6.110	6.189	6.043
1^3D_3	3^-	6.172		6.096	6.145	6.088	6.178	6.188	6.191	6.016
2^3D_1	1^-	6.642		6.527	6.595	6.478	6.542	6.579	6.629	6.362
$2D_2$	2^-	6.650		6.492	6.554	6.422	6.536	6.588	6.651	6.339
$2D'_2$	2^-	6.674		6.542	6.585	6.490	6.542	6.517	6.625	6.320
2^3D_3	3^-	6.687		6.500	6.528	6.429	6.534	6.524	6.637	6.298
3^3D_1	1^-	7.139			6.942					
$3D_2$	2^-	7.147			6.907					
$3D'_2$	2^-	7.167			6.936					
3^3D_3	3^-	7.178			6.885					

Table 6. Leptonic branching fractions of the B meson.

	$B^+ \rightarrow \tau^+ \nu_\tau$ BR_τ	$B^+ \rightarrow \mu^+ \nu_\mu$ BR_μ	$B^+ \rightarrow e^+ \nu_e$ BR_e
this work	0.822×10^{-4}	0.37×10^{-7}	8.64×10^{-12}
PDG [1]	$(1.14 \pm 0.27) \times 10^{-4}$	$< 1.0 \times 10^{-6}$	$< 9.8 \times 10^{-7}$

Table 7. Branching ratio with corresponding rare leptonic decay width of the B^0 meson.

process	$\Gamma(B_q^0 \rightarrow l^+ l^-)/\text{keV}$		BR	
	present	[3]	present	others
$B^0 \rightarrow \mu^+ \mu^-$	4.341×10^{-17}	4.406×10^{-17}	1.002×10^{-10}	$(3.9^{+1.6}_{-1.4}) \times 10^{-10}$ [1] $< 1.1 \times 10^{-9}$ [44] $< 9.4 \times 10^{-10}$ [45] $< 7.4 \times 10^{-10}$ [46] 1.20×10^{-10} [47] $(1.06 \pm 0.09) \times 10^{-10}$ [32] 1.018×10^{-10} [3]
$B^0 \rightarrow \tau^+ \tau^-$	9.097×10^{-15}	9.232×10^{-15}	2.099×10^{-8}	$< 4.1 \times 10^{-3}$ [1] 2.52×10^{-8} [47] $(2.22 \pm 0.19) \times 10^{-8}$ [32] 2.133×10^{-8} [3]
$B^0 \rightarrow e^+ e^-$	1.016×10^{-21}	1.028×10^{-21}	2.345×10^{-15}	$< 8.3 \times 10^{-8}$ [1] 2.82×10^{-15} [47] $(2.48 \pm 0.21) \times 10^{-15}$ [32] 2.376×10^{-15} [3]

Table 8. Branching ratio with corresponding rare leptonic decay width of the B_s^0 meson.

process	$\Gamma(B_q^0 \rightarrow l^+ l^-)/\text{keV}$		BR	
	present	[3]	present	others
$B_s^0 \rightarrow \mu^+ \mu^-$	1.101×10^{-15}	1.583×10^{-15}	2.529×10^{-9}	$(2.9^{+0.7}_{-0.6}) \times 10^{-9}$ [1] $3.0^{+1.0}_{-0.9} \times 10^{-9}$ [44] $3.2^{+1.5}_{-1.2} \times 10^{-9}$ [45] $2.9^{+1.1}_{-1.0} \times 10^{-9}$ [46] 3.40×10^{-9} [47] $(3.65 \pm 0.23) \times 10^{-9}$ [32] 3.602×10^{-9} [3]
$B_s^0 \rightarrow \tau^+ \tau^-$	2.335×10^{-13}	3.361×10^{-13}	5.364×10^{-7}	7.22×10^{-7} [47] $(7.73 \pm 0.23) \times 10^{-7}$ [32] 7.647×10^{-7} [3]
$B_s^0 \rightarrow e^+ e^-$	2.577×10^{-20}	3.695×10^{-20}	5.921×10^{-14}	$< 2.8 \times 10^{-7}$ [1] 7.97×10^{-14} [47] $(8.54 \pm 0.55) \times 10^{-14}$ [32] 8.408×10^{-14} [3]

Table 9. Branching ratio with corresponding radiative leptonic decay width for the B meson.

decay constant	Γ/GeV	BR			
		this work	[48]	[49]	[50]
fp	1.51×10^{-19}	0.38×10^{-6}	0.23×10^{-6}	1.66×10^{-6}	5.21×10^{-6}
$fpcor$	1.36×10^{-19}	0.34×10^{-6}			

3.1 Regge trajectories

The Regge trajectories play a vital role in identifying any new (experimentally) excited state as well as in providing information about the quantum numbers of particular states. We use our predicted ground, radial and orbital excited state masses for the B and Bs mesons to constitute the Regge trajectories for the (n, M^2) and (J, M^2) planes. Here, M stands for the mass of the B and Bs mesons, n stands for the principal quantum number and J is the total spin.

The Regge trajectories with natural ($P=(-1)^J$; $J^P=1^-, 2^+, 3^-$) and unnatural ($P=(-1)^{J-1}$; $J^P=0^-, 1^+, 2^-$) parity in the (J, M^2) plane for the B and Bs mesons are depicted in Figs. 3–6. The masses predicted by our potential model are shown by solid triangles and the experimentally available values by hollow squares with the corresponding meson name. Straight χ^2 fit lines were obtained for the predicted mass values. We have used the following definition

$$J = \alpha M^2 + \alpha_0 \quad (26)$$

to find the slope (α) and the intercept (α_0). The slopes and intercepts for the χ^2 fitted (J, M^2) Regge trajectories are tabulated in Table 10.

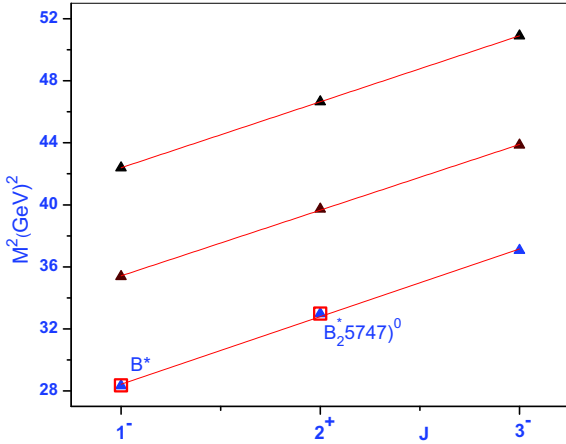


Fig. 3. (color online) Regge trajectory ($M^2 \rightarrow J$) for the B meson with natural parity.

Figures 7 and 8 depict the Regge trajectories using the pseudoscalar ($J^P=0^-$) and vector ($J^P=1^-$) S state, excited P ($J^P=2^+$), D ($J^P=1^-$) and D ($J^P=3^-$) state masses of the B and Bs mesons for $n_r = n - 1$ principal quantum number in the (n_r, M^2) plane. Available experimental values are given by solid dots with the corresponding meson name. Figures 9 and 10 depict the Regge trajectories using the S , P and D state center of weight masses of the B and Bs mesons for $n_r = (n - 1)$ principal quantum number in the (n_r, M^2) plane. We have used the following definition

$$n_r = \beta M^2 + \beta_0 \quad (27)$$

to find the slope (β) and the intercept (β_0). The slopes and intercepts for the χ^2 fitted (n, M^2) Regge trajectories are tabulated in Tables 11 and 12.

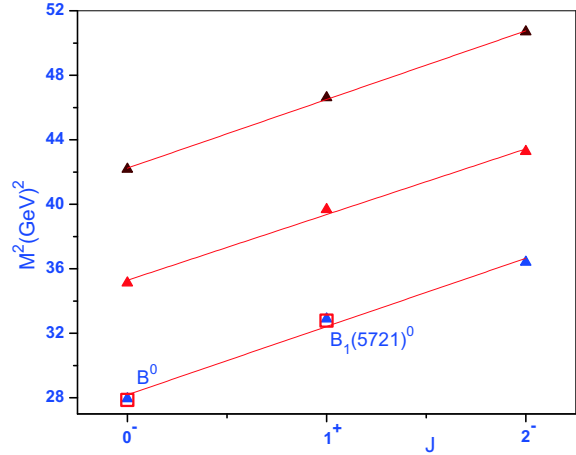


Fig. 4. (color online) Regge trajectory ($M^2 \rightarrow J$) for the B meson with unnatural parity.

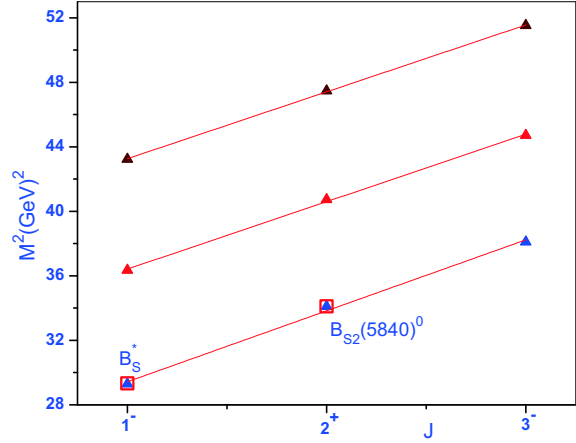


Fig. 5. (color online) Regge trajectory ($M^2 \rightarrow J$) for the Bs meson with natural parity.

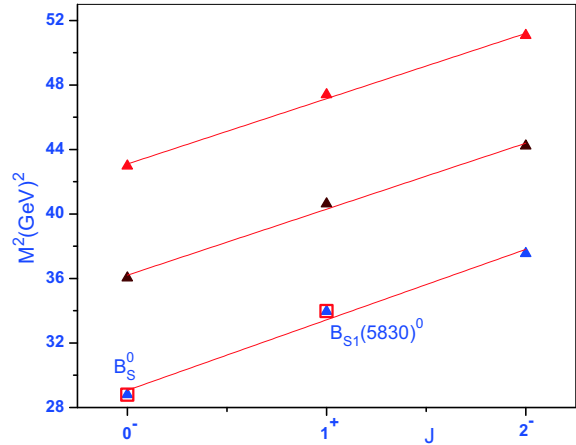


Fig. 6. (color online) Regge trajectory ($M^2 \rightarrow J$) for the Bs meson with unnatural parity.

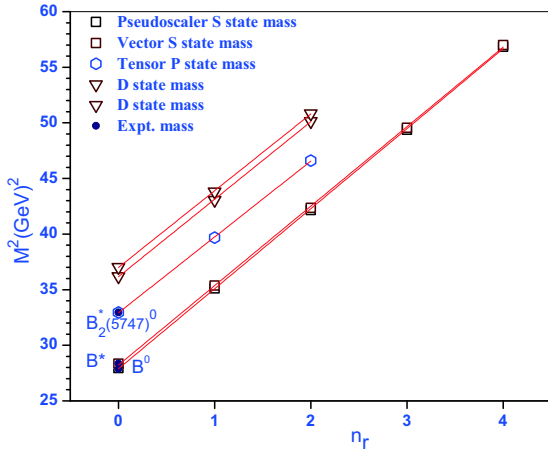


Fig. 7. (color online) Regge trajectory ($M^2 \rightarrow n_r$) for the pseudoscalar and vector S state and excited P and D state masses of the B meson.

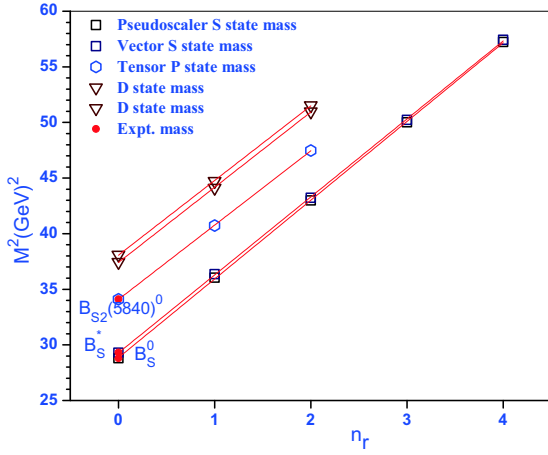


Fig. 8. (color online) Regge trajectory ($M^2 \rightarrow n_r$) for the pseudoscalar and vector S state and excited P and D state masses of the B_s meson.

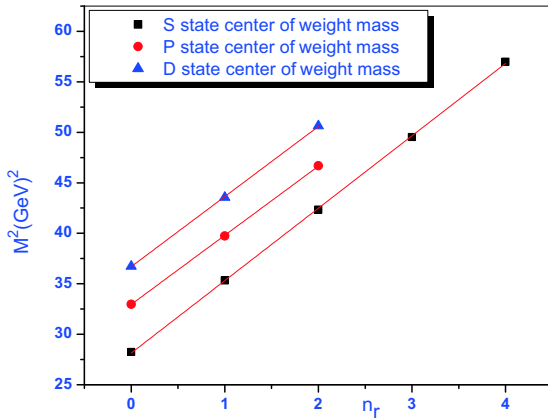


Fig. 9. (color online) Regge trajectory ($M^2 \rightarrow n_r$) for the S-P-D states center of weight mass of the B meson.

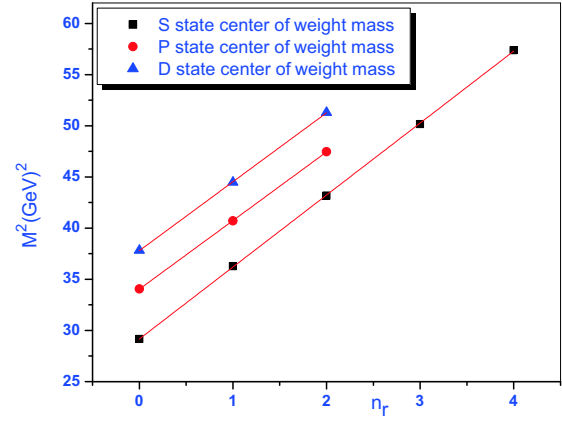


Fig. 10. (color online) Regge trajectory ($M^2 \rightarrow n_r$) for the S-P-D states center of weight mass of the B_s meson.

Table 10. Fitted parameters of the (J, M^2) Regge trajectories with unnatural and natural parity.

parity	meson	trajectory	$\alpha/(\text{GeV}^{-2})$	α_0
unnatural	$B(b\bar{q})$	parent	0.234 ± 0.022	-6.576 ± 0.741
		first daughter	0.244 ± 0.016	-8.616 ± 0.634
		second daughter	0.235 ± 0.005	-9.813 ± 0.261
	$b_s(b\bar{s})$	parent	0.226 ± 0.023	-6.565 ± 0.791
		first daughter	0.243 ± 0.017	-8.789 ± 0.702
		second daughter	0.246 ± 0.013	-10.605 ± 0.611
natural	$b^*(c\bar{q})$	parent	0.229 ± 0.008	-5.500 ± 0.277
		first daughter	0.236 ± 0.003	-7.353 ± 0.128
		second daughter	0.235 ± 0.0004	-8.856 ± 0.021
	$b_s^*(c\bar{s})$	parent	0.226 ± 0.012	-5.665 ± 0.407
		first daughter	0.239 ± 0.006	-7.701 ± 0.265
		second daughter	0.241 ± 0.003	-9.425 ± 0.149

Table 11. Fitted slope and intercept for the (n_r, M^2) Regge trajectories.

meson	state	J^P	$\beta/(\text{GeV}^{-2})$	β_0
B	S	0^-	0.139 ± 0.0008	-3.873 ± 0.037
	S	1^-	0.139 ± 0.001	-3.946 ± 0.045
	P	2^+	0.146 ± 0.001	-4.822 ± 0.047
	D	1^-	0.143 ± 0.001	-5.182 ± 0.057
	D	3^-	0.144 ± 0.001	-5.357 ± 0.067
B_s	S	0^-	0.141 ± 0.0006	-4.071 ± 0.026
	S	1^-	0.142 ± 0.0006	-4.173 ± 0.028
	P	2^+	0.149 ± 0.0007	-5.097 ± 0.030
	D	1^-	0.147 ± 0.001	-5.526 ± 0.051
	D	3^-	0.149 ± 0.001	-5.669 ± 0.057

Table 12. Fitted parameters of Regge trajectory (n_r, M^2) for the S - P - D states center of weight mass.

meson	trajectory	$\beta/(\text{GeV}^{-2})$	β_0
$B(b\bar{q})$	S state	0.139 ± 0.001	-3.922 ± 0.042
	P state	0.145 ± 0.001	-4.810 ± 0.042
	D state	0.143 ± 0.001	-5.283 ± 0.061
$B_s(b\bar{s})$	S state	0.142 ± 0.0006	-4.147 ± 0.027
	P state	0.149 ± 0.0006	-5.075 ± 0.024
	D state	0.148 ± 0.0012	-5.609 ± 0.054

With a comparison of the slopes, the slope values α are larger than the slope values β . The ratio of the mean of α and β is 1.68 and 1.62 for the B and B_s meson respectively. The estimated masses of the B and B_s mesons fit well to the linear trajectories in the (n, M^2) and (J, M^2) planes and are almost parallel to and equidistant from each other. With the help of the Regge trajectories, we can identify any new (experimentally) excited states as well as ascertain information about quantum number of the state.

4 Conclusion

Our predicted masses for the S - P - D states of the B and B_s mesons are very close to the available experimental values. The excited state ($4S$, $5S$, $3P$ and $3D$) masses are higher than other theoretical estimates. The estimated relativistic correction to the kinetic energy term is found to be less than 1%, while that of the potential energy term is found to be around 3%–5%. With limited experimental observations of excited states of the B and B_s mesons, the LHCb collaboration's recent measure-

ments show the possibility of updating our knowledge of the excited states of these mesons. For the B meson, the 1P states $B_1(5721)$ and $B_2^*(5747)$ are in good agreement with our prediction [1, 6]. We have assigned newly observed states $B(5970)$ [42] to the 2^3S_1 state of the B meson. For the B_s meson, the 1P experimental states $B_{S1}^*(5830)$ and $B_{S2}^*(5840)$ are in excellent agreement with our predicted values. These are only a few excited state measurements, but in the near future LHCb should provide new results in bottom meson spectroscopy.

The Regge trajectories for the B and B_s mesons in both (J, M^2) and (n_r, M^2) planes are almost linear, equidistant and parallel. Regge trajectories provide information about the quantum numbers of a given state and are useful to identify any new excited state (experimentally). From Figs. 3–6, we found that the experimental states are sitting nicely on straight lines without deviation.

The pseudoscalar decay constants with QCD correction for both mesons are underestimated compared to other theoretical model estimates. Our calculated leptonic branching fractions of the B meson are fairly close to the PDG [1] values. Our calculated radiative leptonic branching ratio of the order of 10^{-6} is in good agreement with the branching ratio obtained with the form factor parameterizing approach [48]. The estimated rare leptonic decay widths as well as the branching ratios of the B and B_s mesons have been compared with experimental observations and other theoretical estimates [3, 44, 46, 47], and the results are in good agreement (see Tables 7 and 8).

Finally, this study may help current experimental facilities to identify new states of the B and B_s mesons as well as their J^{PC} values.

References

- 1 C. P. et al (Particle Data Group), Chinese Physics C, **40**: 100001 (2016)
- 2 Q. F. Lu, T. T. Pan, Y. Y. Wang, E. Wang, and D. M. Li, Phys. Rev. D, **94**(7): 074012 (2016)
- 3 M. Shah, B. Patel, and P. Vinodkumar, Phys. Rev. D, **93**(9): 094028 (2016)
- 4 J. B. Liu, C. D. Lu, arXiv:1605.05550 [hep-ph] (2016)
- 5 J. B. Liu, M. Z. Yang, Chin. Phys. C, **40**(7): 073101 (2016)
- 6 R. Aaij et al, JHEP, **04**: 024 (2015)
- 7 H. X. Chen, W. Chen, X. Liu, Y. R. Liu, and S. L. Zhu, Rept. Prog. Phys., **80**: 076201 (2017), 1609.08928
- 8 S. Godfrey, N. Isgur, Phys. Rev. D, **32**: 189 (1985)
- 9 P. Colangelo, F. De Fazio, and G. Nardulli, Phys. Lett. B, **316**: 555 (1993)
- 10 M. Di Pierro, E. Eichten, Phys. Rev. D, **64**: 114004 (2001)
- 11 M. Z. Yang, Eur. Phys. J. C, **72**: 1880 (2012)
- 12 D. Ebert, R. Faustov, and V. Galkin, Eur. Phys. J. C, **71**: 1825 (2011)
- 13 A. M. Eisner, *Recent Results on Radiative and Electroweak Penguin Decays of B Mesons at BaBar*, in (DPF 2013), USA, August 13-17, (2013)
- 14 D. Ebert, R. Faustov, and V. Galkin, Eur. Phys. J. C, **66**: 197 (2010)
- 15 J. C. Yang, M. Z. Yang, Mod. Phys. Lett. A, **27**: 1250120 (2012)
- 16 S. N. Gupta, J. M. Johnson, Phys. Rev. D, **51**(1): 168 (1995)
- 17 D. S. Hwang, C. Kim, and W. Namgung, Phys. Lett. B, **406**: 117 (1997)
- 18 V. Kher, N. Devlani, A. K. Rai, (2017), 1704.00439
- 19 Y. Koma, M. Koma, and H. Wittig, Phys. Rev. Lett., **97**: 122003 (2006)
- 20 E. Eichten, K. Gottfried, T. Kinoshita, K. D. Lane, and T. M. Yan, Phys. Rev. D, **17**(11): 3090 (1978)
- 21 N. Devlani, A. K. Rai, Int. J. Theor. Phys., **52**: 2196 (2013) ISSN 0020-7748
- 22 N. Devlani, A. K. Rai, Phys. Rev. D, **84**: 074030 (2011)
- 23 A. K. Rai, B. Patel, and P. C. Vinodkumar, Phys. Rev. C, **78**(5): 055202 (2008)
- 24 A. K. Rai, R. H. Parmar, and P. C. Vinodkumar, J. Phys. G: Nucl. Part. Phys., **28**(8): 2275 (2002)
- 25 E. J. Eichten, C. Quigg, Phys. Rev. D, **49**(11): 5845 (1994)
- 26 D. Gromes, Z. Phys. C, **26**: 401 (1984)
- 27 S. Gershtein, V. Kiselev, A. Likhoded, and A. Tkabladze, Phys.

- Usp., **38**: 1 (1995)
- 28 S. Godfrey, K. Moats, and E. S. Swanson, Phys. Rev. D, **94**(5): 054025 (2016)
- 29 T. Barnes, N. Black, and P. R. Page, Phys. Rev. D, **68**: 054014 (2003)
- 30 D. Silverman, H. Yao, Phys. Rev. D, **38**(1): 214 (1988)
- 31 C. D. Lu, G. L. Song, Phys. Lett. B, **562**: 75 (2003)
- 32 C. Bobeth, M. Gorbahn, T. Hermann, M. Misiak, E. Stamou, and M. Steinhauser, Phys. Rev. Lett., **112**: 101801 (2014)
- 33 C. Bobeth, M. Gorbahn, and E. Stamou, Phys. Rev. D, **89**(3): 034023 (2014)
- 34 G. Buchalla, A. J. Buras, Nucl. Phys. B, **400**: 225 (1993)
- 35 A. J. Buras, in *Weak Hamiltonian, CP violation and rare decays*, Proceedings, France, July 28-September 5, 1997. Pt. 1, 2 (1998), pp. 281–539
- 36 H. S. Lee, $\sin^2\theta_W$ theory and new physics, in *10th International Workshop on e^+e^- collisions from Phi to Psi (PHIPSI15)*, China, September 23-26, 2015
- 37 R. Van Royen, V. Weisskopf, Nuovo Cim. A, **50**: 617 (1967)
- 38 E. Braaten, S. Fleming, Phys. Rev. D, **52**(1): 181 (1995)
- 39 Y. Sun, Q. T. Song, D. Y. Chen, X. Liu, and S. L. Zhu, Phys. Rev. D, **89**(5): 054026 (2014)
- 40 N. Devlani, A. Rai, Eur. Phys. J. A, **48**: 104 (2012)
- 41 T. Lahde, C. Nyfalt, and D. Riska, Nucl. Phys. A, **674**: 141 (2000)
- 42 T. A. Aaltonen et al, Phys. Rev. D, **90**(1): 012013 (2014)
- 43 T. Affolder et al (CDF), Phys. Rev. D, **64**: 072002 (2001)
- 44 S. Chatrchyan et al, Phys. Rev. Lett., **111**: 101804 (2013)
- 45 R. Aaij et al (LHCb), Phys. Rev. Lett., **110**(2): 021801 (2013)
- 46 R. Aaij et al (LHCb), Phys. Rev. Lett., **111**: 101805 (2013)
- 47 P. Dimopoulos et al (ETM), JHEP, **01**: 046 (2012)
- 48 G. P. Korchemsky, D. Pirjol, and T. M. Yan, Phys. Rev. D, **61**: 114510 (2000)
- 49 J. C. Yang, M. Z. Yang, Nucl. Phys. B, **889**: 778 (2014)
- 50 J. C. Yang, M. Z. Yang, Nucl. Phys. B, **914**: 301 (2017)
- 51 D. Atwood, G. Eilam, A. Soni, Mod. Phys. Lett. A, **11**: 1061 (1996)
- 52 J. C. Yang, M. Z. Yang, Mod. Phys. Lett. A, **31**(03): 1650012 (2015)
- 53 V. Khachatryan et al, Nature, **522**: 68 (2015)